Materials Research Proceedings 28 (2023) 869-878 https://doi.org/10.21741/9781644902479-95

Galling-free fine blanking of titanium plates by carbon-supersaturated tool steel punch

AIZAWA Tatsuhiko[1,a *], FUCHIWAKI Kenji[2,b] and DOHDA Kuniaki[3,c]

[1]Shibaura Institute of Technology, 3-15-10 Minami-Rokugo, Ota-City, Tokyo 144-0045, Japan

[2]Hatano Seimitsu Co, 183-7 Hirasawa, Hatano-City, Kanagawa 257-0015, Japan

[3]Northwestern University, Evanstone, IL 60268, USA

[a]taizawa@sic.shibaura-it.ac.jp, [b]kenji-fuchiwaki@hatanoseimitsu.co.jp, [c]dohda.kuni@northwestern.edu

Keywords: Forging, Fine Blanking, Galling Free, Titanium, Carbon-Supersaturation, Tool Steel Punch, High-Speed Steel Punch, In Situ Solid Lubrication

Abstract. The carbon supersaturated tool steel and high-speed steel punches were utilized to demonstrate that the titanium work materials were forged in high reduction of thickness and fine-blanked without adhesion of their fragments and deposition of their oxide debris particle. This galling free forging and fine blanking came from the in situ formation of the free carbon tribofilm only on the highly stressed interfaces between the punch/die and the titanium work. Under this in situ solid lubrication, the low frictional state was sustained to induce less bulging deformation of work during the forging process. The fine blanking of titanium plates advanced without adhesive wear and fractured regions on their sheared surface. The long life of tools was certified even in fine blanking of titanium and titanium alloy plates.

Introduction

Titanium and titanium alloys have been utilized as typical high strength, light-weight and bio-compatible structural materials in the aerospace industries [1], in the medical applications [2] and in the mechanical part-markets [3]. For manufacturing of those parts and members, various metal forming processes, such as forging, drawing and fine blanking, are utilized to shape their feedstock like bars, plates and billets into products. As reported in [4-5], those processes encountered severe wears by adhesion of fresh titanium fragments and by deposition of titanium oxide debris particles onto the punches and dies. In practical operations during forming the titanium alloy bar to its glass-frames, the cleansing and polishing steps must be included to eliminate the adhesive films and to clean up the debris particles between the successive forging steps under the limited reduction of thickness [4]. In addition, as studied in [5-7], the ceramic dies and their coatings and DLC (Diamond Like Carbon) coatings, were also subjected to highly frictional state with metal sticking during the deep drawing process and in the BOD (Ball-On-Disk) testing in dry, respectively. In particular, TiAlN, TiN and TiCN experienced extremely high friction and seizure against the pure titanium balls.

The pretreatment of SKD11 and AISI420 punches and dies by the low temperature plasma carburizing, played a significant role in dry and cold forging of the pure titanium and β-titanium alloy wires [8-9]. No galling or no adhesion wear occurred in those forging steps even in high reduction of thickness. As explained in detail [10], this anti-galling behavior in metal forming of titanium bars was attributed to in situ formation of free carbon tribofilms onto the highly stressed contact interface of punches and dies to the titanium works during forming process. In addition, this galling-free forging process was characterized by the low friction and low work-hardening even in higher reduction of thickness than 70% [11-12]. This pretreatment to punches and dies are

attractive to the near-net shaping by forging steps in galling-free and to the fine-blanking with fully burnished surface.

In the present paper, the carbon supersaturated (CS-) tool steel and high-speed steel punches are prepared by the low temperature plasma carburizing. This CS-SKD11 punch and die is utilized to upset the pure titanium bar till the reduction of thickness reaches 70%. The loading - displacement curves are online monitored to describe the compressive and flattening deformation of titanium work. The homogeneous flattening deformation proves that the low frictional state is preserved during forging. The CS-YXR high-speed steel punch is also prepared for fine blanking the pure titanium plates. The normal YXR punch suffers from severe adhesion of titanium fresh surfaces even in a single shot. The punch edges and side surfaces are completely adhered and eroded by the titanium fragments. On the other hand, no galling occurs on the CS-YXR punch edge and side surfaces even after fine blanking the titanium plates repeatedly. This significant difference in galling behavior proves the effectiveness of carbon supersaturation to steel punches and dies for fine blanking the difficult-to-metal-forming work materials.

Methods and Materials

The plasma carburizing system for carbon supersaturation process is first explained with notes on the plasma processing setup and conditions with reference to the previous studies in the literature. The forging and fine blanking setups and systems are also stated with comments on the extension of laboratory-scale methods to the mass production in industries.

Carbon supersaturation process.

The plasma carburizing system was schematically illustrated in Fig. 1a. With reference to the previous studies in [13-14], the hollow cathode device was employed to increase the carbon-ion and CH-radical densities more than 3 x 10^{17} ions/m^3 and to deepen the carbon supersaturated layer thickness. It was estimated to be 40 μm in case of the plasma carburizing at 673 K for 14.4 ks by 70 Pa.

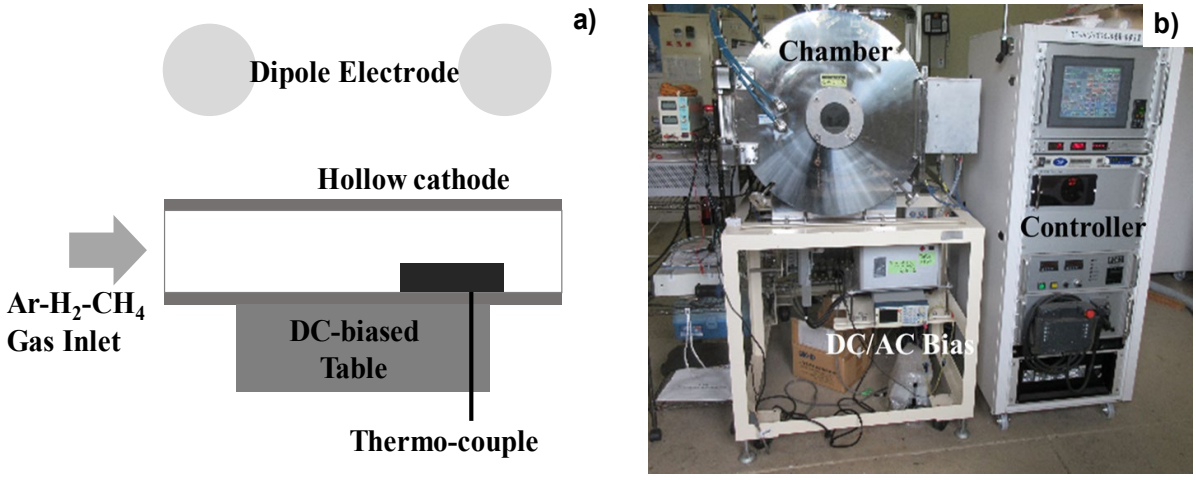

Fig. 1. Low temperature plasma carburizing system. a) Schematic view on the experimental setup, and b) overview on the whole system.

The dipole electrodes were utilized to ignite the RF (Radio-Frequency) plasma while the DC (Direct Current) plasma was also induced by applying the bias voltage to the bottom of hollow cathode. In the following experiments, the RF-voltage and the DC-bias were constant by +220 V and -400 V, respectively. After evacuation down to the base pressure of 0.01 Pa, the argon gas was introduced to a chamber in Fig. 1b at RT to clean the punch and die surfaces. After increasing the process temperature up to 673 K under the argon atmosphere, the hydrogen gas was

also introduced with the argon gas with the flow rate of 160 mL/min for argon and 20 mL/min, respectively. The total pressure was constant by 70 Pa. After presputtering by the DC-plasmas for 1.8 ks, the methane gas was introduced as a carbon source into argon and hydrogen mixture gas by the flow rate of 20 mL/min. At the specified duration of 14.4 ks, the specimen was cooled down in the chamber under the nitrogen atmosphere before evacuation down to atmospheric pressure. The processing temperature was in situ monitored by the thermocouple, which was embedded into the base plate below the hollow cathode device in Fig. 1a. The total pressure and each flow rate of argon, hydrogen and methane gasses were also measured for process control. The deviation of temperature and pressure in operation was ± 0.1 K and ± 0.05 Pa, respectively. After [8, 11-12], no iron and chromium carbides were synthesized in the plasma-carburized layer. The peak shift of α-ion to the lower 2θ angles in XRD analysis revealed that the α-lattices in the carburized SKD11 layer expanded by themselves through supersaturation of carbon solutes into steel substrates. The maximum surface roughness of punches at 5 mm away from their edge was 0. 35 μm before carburizing and 0.366 μm after carburizing. Hardness of SKD11 punch increased from 700 HV to 950 HV.

Forging process.

The CNC stamping system (ZEN-04; Hoden-Seimitsu, Co., Ltd., Kanagawa, Japan) was used for forging the pure titanium wire with the diameter of 1.0 mm in dry at the room temperature. The load to stroke curves were measured in every reduction of thickness by the load cell, which was embedded into the lower die in Fig. 2a. The overview of this stamping system was depicted in Fig. 2b. No lubricating oils and solid lubricants were utilized in the forging experiments. The punching speed was constant by 1 mm/s.

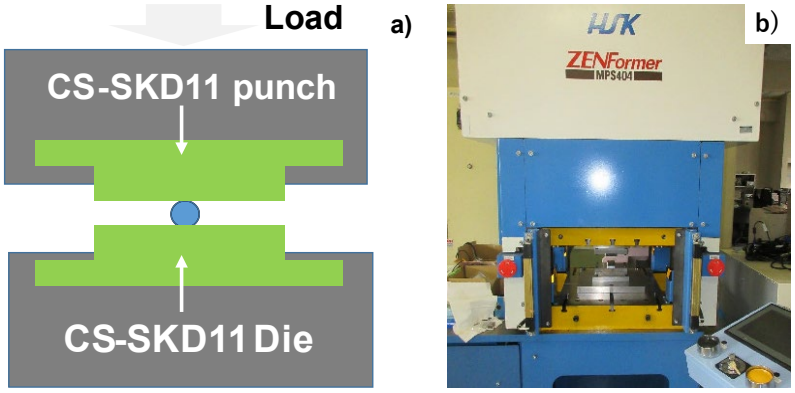

Fig. 2. CNC forging system. a) Schematic view on the forging experimental setup, and b) overview on the whole forging system.

Fine blanking process.

The pure titanium plate with the thickness of 2.0 mm, was blanked with narrow clearance of 4% at the room temperature as illustrated in Fig. 3a. The mechanical stamper (FB 160-FDE; Mori Steel Works Co., Ltd.; Saga, Japan), specially accommodated for fine-blanking process was used for this experiment as shown in Fig. 3b. The punching speed was 5 mm/s.

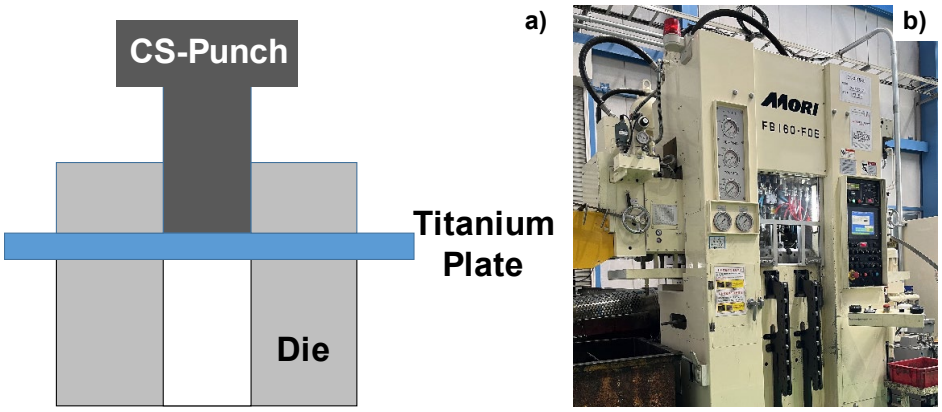

Fig. 3. Fine blanking system. a) Schematic view on the fine-blanking experimental setup, and b) overview on the whole system.

The maximum loading capacity was 1600 kN. The loading sequence for fine blanking was CNC-programmed. The punch with and without carbon-supersaturation were employed to describe the effect of carbon supersaturation on the galling behavior. Each punch was fixed into the punch holder, which was further set up into the upper die set. In the following experiments, FBH9-HMC with the viscosity of 101 m^2/s was utilized as a lubricating oil.

Work and tool materials.

Pure titanium wires and plates were respectively utilized as a work material for upsetting and fine blanking experiments. Their chemical composition consists of hydrogen by 0.0012 mass%, oxygen by 0.097 mass%, nitrogen by 0.007 mass%, iron by 0.042 mass%, carbon by 0.007 mass%, and titanium for balance. A tool steel type SKD11 (or AISI/SAE D3) was employed as a punch material for forging. A high-speed steel type YXR7 was used as a punch for fine blanking. Their chemical compositions were listed in Table 1.

Table 1. Chemical composition of SKD11 and YXR7 punch substrates.

Punch	C	Si	Mn	P	S	Cr	Mo	V	W	Fe
SKD11	1.44	0.3	0.35	0.27	0.06	11.1	0.8	0.2	---	in balance
YXR7	0.8	0.8	0.3	---	---	4.7	5.5	1.3	1.3	in balance

Characterization.

SEM (Scanning Electron Microscopy) - EDX (Energy Dispersive X-ray spectroscopy) was used for microstructure analysis and element mapping on the contact interface of forging and fine-blanking tools to the titanium work materials. Raman spectroscopy (JOEL, Co., Ltd.; Kanagwa, Japan) was also utilized to characterize the binding state of tribofilms.

Results

CNC-stamping was first utilized to describe the upsetting behavior of pure titanium bar with increasing the reduction of thickness. SEM-EDX and Raman spectroscopy were used to analyze the contact interface between the CS-SKD11 punch and the titanium work. Fine blanking system was also utilized to describe the difference of YXR7 punch surface with and without the carbon supersaturation to the fine-blanking punch.

Forging of pure titanium by CS-SKD11 punch.

The pure titanium bar with the diameter of 1.0 mm was upset to the specified reduction of thickness (r), using the CS-SKD11 punch and die. Figure 4 depicts the variation of contact interface width (Wi) with increasing r. When $r < 30\%$, Wi is less than the upset bar width (Wo); e.g., when $r = 20\%$, Wo = 1.15 mm and Wi = 0.70 mm. However, when $r > 50\%$, this Wi

Materials Research Proceedings 28 (2023) 869-878 https://doi.org/10.21741/9781644902479-95

approaches to Wo; e.g., when r = 50%, Wo = 1.7 mm and Wi = 1.5 mm. This reveals that the bulging deformation is suppressed with increasing r and the upset titanium bar homogeneously flattens with r.

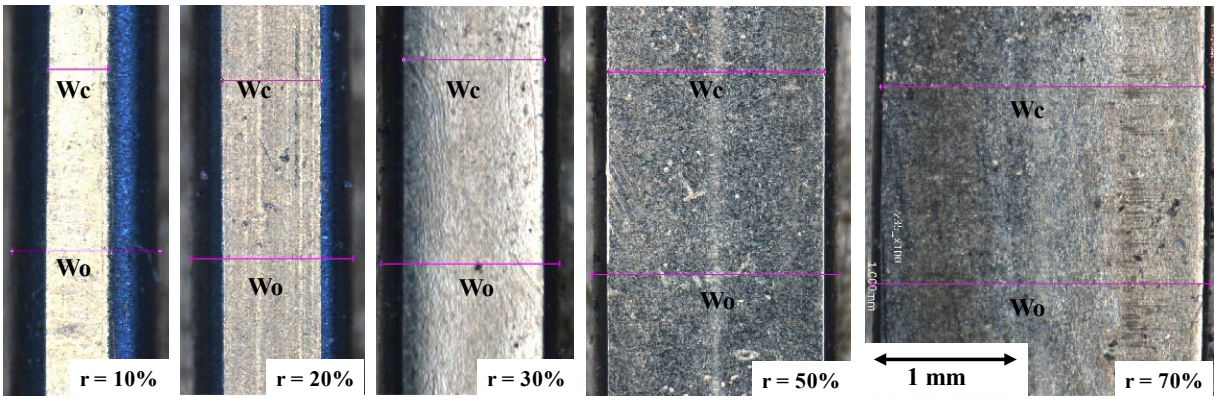

Fig. 4. Variation of the contact interface width at each reduction of thickness by r = 10%, 20%, 30%, 50% and 70% during the upsetting with the use of CS-SKD11 punch and die.

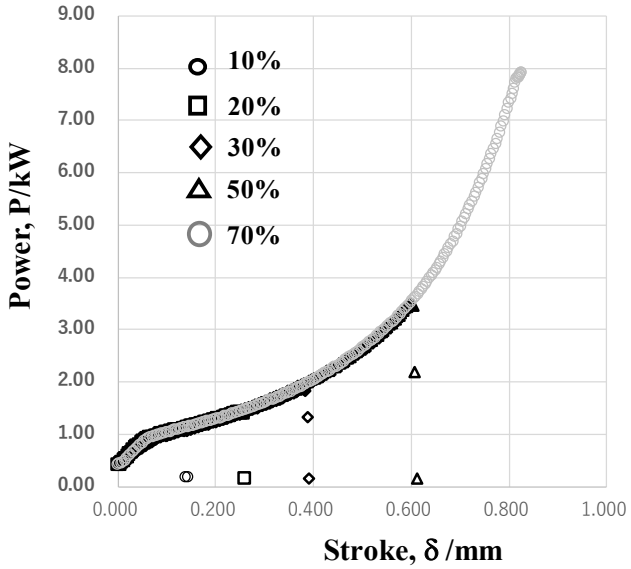

Fig. 5. The measured forging load to stroke relationship at each reduction of thickness for r = 10%, 20%, 30%, 50% and 70%, respectively.

After the empirical relationship between the friction coefficient (μ) and the bulging deformation ratio (= (Wo-Wi)/(2Wo)) in [15], μ is estimated to be 0.05 to 0.1. After the inverse analysis on the friction coefficient using the finite element simulation in [11], μ is estimated to be 0.05. Under this low friction on the interface between the CS-SKD11 punch and the pure titanium works, its thickness is homogeneously upset to r = 70%.

The in-situ measured forging load was plotted against the applied stroke at each reduction of thickness. As depicted in Fig. 5, every load-stroke curve at r = 10%, 20%, 30%, 50% and 70% is edited to one master load-stroke relationship. This implies that the pure titanium work homogeneously deforms with increasing the stroke, irrespective of the reduction of thickness. The forging load abrupt increases in the exponential manner with the stroke when r > 30%. This reveals that the true contact interface area expands by flattening behavior in Fig. 4.

The low friction on the contact interface as well as the homogeneous forging behavior proves that no galling occurs during this forging process with high reduction of thickness. Through the

precise analysis on the contact interface, the interfacial state is described after upsetting the pure titanium bars up to r = 70% in twenty shots.

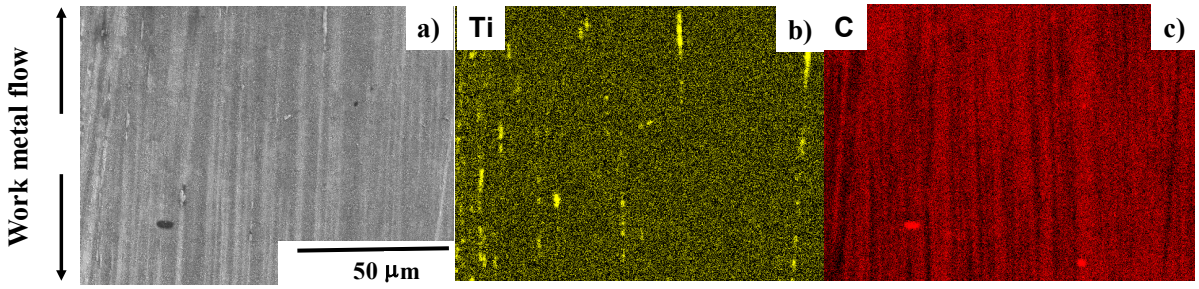

Fig. 6. SEM image and element mapping on the true contact interface between the CS-punch and the pure titanium work after continuously forging up to r = 70% in twenty shots.

As shown in Fig. 6a, many gray stripes are formed on the interface along the direction of work metal flow. Since the CS-punch surface was cleansed and polished before experiment, no surfactants and residuals were left on the punch and die surfaces. Hence, these stripes were in situ formed during the forging steps. SEM-EDX analysis was used to search for the element mapping in correspondence to these stripes among the main constituent elements of SKD11 such as iron and chromium, the titanium, the oxygen and the carbon. The iron and chromium maps were the same as before forging experiments; no correlations to SEM image in Fig. 6a were noticed. As shown in Fig. 6b, several thin titanium stripes were seen together with the oxygen mapping. There was no significant correlation to the SEM image. Figure 6c shows the carbon mapping on the interface; the gray stripes are carbon films, in situ formed onto the contact interface between the CS-SKD11 punch and the titanium work during the forging process.

This SEM-EDX analysis on the contact interface of CS-SKD11 punch to the titanium work proves that the in-situ formed free carbon tribofilm works as a solid lubricant medium on the true contact interface to lower the friction coefficient and to make homogeneous metal flow along the CS-punch interface. Nearly the same in situ solid lubrication was also observed on the contact interface between CS-die and the titanium work. These low frictional state of punch and die as well as the smooth work flow along their interfaces, characterizes the galling-free forging behavior when using the carbon supersaturated special tools.

To be noticed, no carbon maps in stripes in Fig. 6 were detected outside of the true contact area on the CS-punch and CS-die surfaces. That is, the applied stresses working on the true contact interface are necessary to in situ form the free carbon tribofilm. High compressive normal stress induces the diffusion of carbon solutes in the CS surface zones to the true contact interfaces of punch and die so that these free carbon agglomerates form the carbon tribofilm only on the contact interface.

Fine blanking of pure titanium by YXR punch.

In the fine blanking, the punch head is subjected to high normal stresses when punching out the work materials under the narrow clearance between the punch and die. The punch edge experiences the high shear stress transients and local metal flow change. The punch side surfaces are also subjected to shearing flow of work materials. Under these mechanical conditions with more severity than forging, the plastic distortion of work materials could result in galling damage on the XYR7 punches when fine-blanking the ductile and high-strength stainless steel and titanium plates.

In the present experiment, a bare YXR7 punch was used as a reference to describe the galling behavior when fine-blanking the pure titanium plate with the thickness of 2 mm in a single shot under the lubricating conditions. The CS-YXR7 was also utilized to demonstrate the role of carbon supersaturation in galling-free fine blanking.

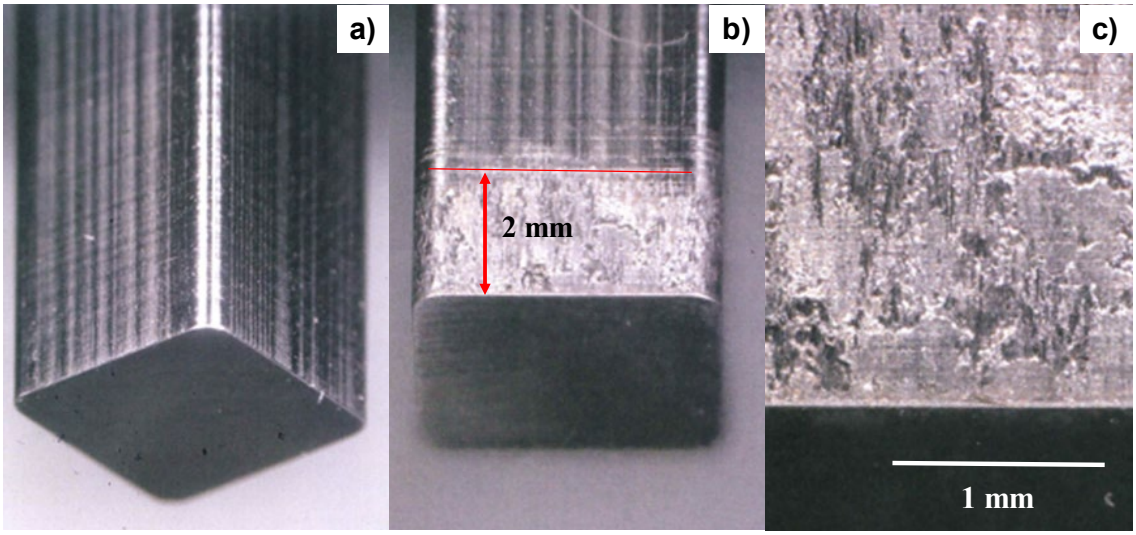

Fig. 7. YXR7 fine-blanking punch before and after fine blanking the pure titanium plate with the thickness of 2.0 mm in a single shot. a) YXR7 punch before fine blanking test, b) YXR7 punch after fine blanking test, and c) adhesion layer on the punch side surfaces.

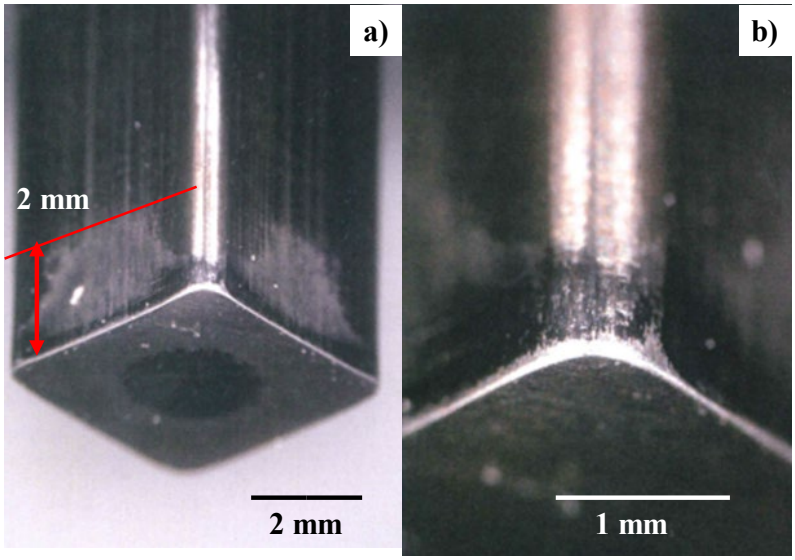

Fig. 8. CS-YXR7 punch after successively fine blanking the austenitic stainless steel AISI304 plates in three shots and the pure titanium plates in two shots. a) CS-YXR7 punch after fine blanking test, and b) punch surfaces around its edge and corner.

Fig. 7a and 7b compare the YXR7 punch surfaces before and after fine blanking the pure titanium plate with the thickness of 2.0 mm. No wears were seen both on the punch head after fine blanking in a single shot. However, its side surfaces with the length around 2 mm were almost covered by the fragments of titanium work. In particular, as seen in Fig. 7c, the titanium fragments adhered and eroded into the YXR7 punch., resulting in total failure of punch. This galling behavior proves that the fresh sheared titanium work is easy to adhere onto the punch side surfaces in the high normal and shear stress conditions under the narrow clearance.

Fine blanking of pure titanium by CS-YXR punch.

CS-YXR7 punch was used to make fine blanking the AISI316 plates with the thickness of 3 mm in three shots and then to punch out the pure titanium plate with the thickness of 2 mm in two shots. Fig. 8a shows the overview of CS-YXR7 after a series of fine blanking shots.

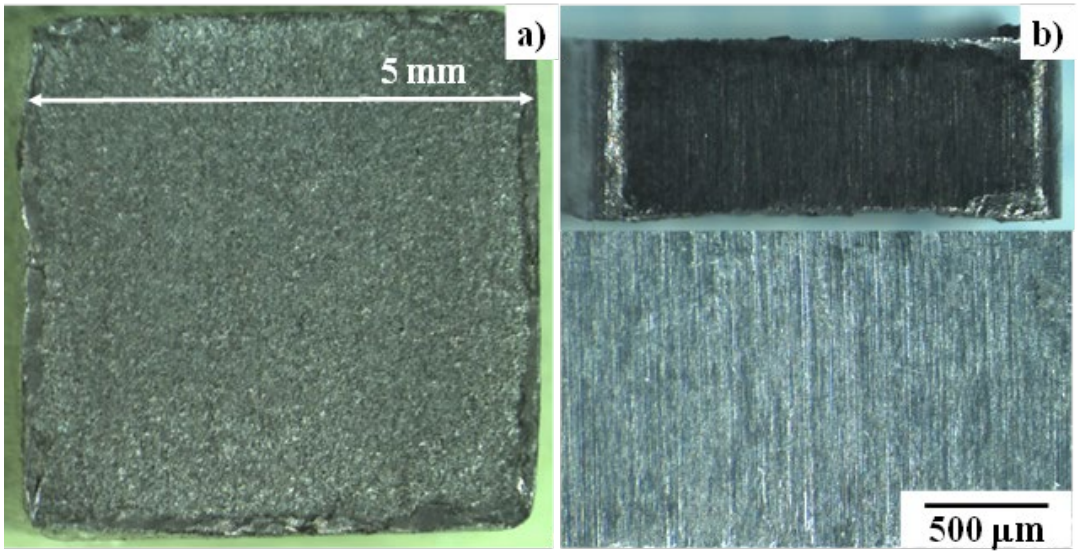

Fig. 9. The side and bottom surface of titanium blank, punched pout by the CS-YXR7 punch.

In contrast to the severe adhesion of titanium fragments onto the bare YXR7 punch in Fig. 8b and 8c, the CS-XYR7 punch is completely free from the galling of sheared titanium work even after punching the stainless steel and titanium plates in several times. This implies that in situ formed free carbon tribofilms are formed on the highly stressed contact surfaces of punch under the narrow clearance in the similar manner to the in situ solid lubrication as seen in Figure 6 when forging the pure titanium plate. Once the tribofilm is formed on the fine blanking punch, no adhesive wear of metal works occurs even with increasing the number of shots.

This galling-free behavior suggests that the quality of punched-out blank is expected to be improved by this fine blanking process. Fig. 9 depicts the top and side surfaces of punched-out titanium blank. No fractured regions are detected on every four side surface of blank. This proves that CS-YXR7 punch is suitable to high qualification in fine blanking of titanium plates to products.

Discussion

The flash temperature on the highly stressed contact interface between the punches/dies and the work materials was thought as a main process parameter to govern the galling heavier in forging [7, 16]. In fact, the oxidation wear of carbon-based coatings such as diamond and DLC (Diamond Like Carbon) in stamping and forging [17] suggested that the chemical galling had overwhelming influence on the abrasive wear of tool surfaces at hot spots. As compared in Figs. 7 and 8, the active metals such as pure titanium with chemical compatibility to various inorganic materials, induced the adhesive wear onto the steel tool surfaces at RT even under the lubricating conditions. This mechano-chemically adhesive galling under highly stressed condition, accompanied with erosion of titanium into the tools. Under the free carbon tribofilms, in-situ formed onto the carbon supersaturated SKD11 and YXR7 punches, this adhesive galling is completely suppressed to make forging and fine-blanking repeatedly without metallic sticking and seizure. This reveals that inactive tribofilm is needed to be free from the mechano-chemical adhesion galling.

As had been discussed in the dry tribological behavior of carbon-based coatings [6-7], the high friction coefficient, experienced in the TiN, TiCN, TiAlN and other ceramic coatings, much reduced in the silicon-bearing DLC and nano-laminated DLC coatings during the BOD testing. This implies that adhesive galling is effectively suppressed on the bound carbon surface of the amorphous carbon microstructure. In the present in-situ solid lubrication, the free carbon film with nearly the same Raman spectroscopy as the hydrogenated DLC (or a:C:H) works as an inactive buffer interface between the fresh titanium and the steel punch.

Let us consider the effect of carbon bound state on the frictional behavior. Although the SKD11 houses the iron and chromium carbides by heat treatment and the YXR7 has a low carbon content, severe galling occurs as seen in Fig. 7. The bound carbon in the carbides and the alloying carbon element have no capacity of in situ solid lubrication. The weakly bound carbon in the amorphous carbon film has a little capacity to reduce the friction under mild tribological conditions. The unbound carbon tribofilm has a significant capacity to be free from mechano-chemical adhesion wears in fine blanking. This difference in the bound state of carbons on the contact interface, directly reflects on the galling process of titanium works.

As keenly discussed in [10] and suggested in [18-19], the supersaturated carbon in the steel punches diffuses onto the contact interface to titanium work under high stress gradient, and, forms a free-carbon tribofilm. As seen in Figs. 4 and 8a, no tribofilms were formed outside of the true contact area. In case of forging process, the carbon stripes were formed as a thin tribofilm on the true contact interface of CS-SKD11 punch to titanium work. In case of fine blanking, the carbon film was also formed as a thin tribofilm on the contact interface of CS-YXR7 punch. Remember that high normal stress was applied onto the contact interface when forging the pure titanium wire, and that higher normal stress and high shear stress were combined and applied onto the contact interface when fine-blanking the pure titanium plate. This reveals that tribofilm thickness is dependent on the applied stress level during metal forming processes. To be noticed, the free-carbon tribofilm formed onto the YXR7 punch surface is so tough not to be delaminated even in high and combined stress conditions without galling. Owing to this in situ formation of tough tribofilm, the CS-YXR7 punch is also free from adhesive wearing even with increasing the number of shots as discussed in [20]. This carbon supersaturation into punch and die substrates are necessary to prolong the tool life without severe galling in the fine blanking of titanium plates.

As reported in [21-22], the abrasive and adhesive galling processes were effectively suppressed by the nanotexturing onto the punch side surface when punching out the electrical steel sheets. This was because the debris particles were ejected through the nanotextured grooves to the outside of punching process. This nanotexturing effect can be also accommodated to this fine blanking with the use of CS-steel punches. The titanium and titanium alloys parts with fully burnished surface can be near-net shaped by this fine blanking without significant galling and abrasive wear. The effect of galling-free fine blanking on the product quality and tool life is a next issue to advance this new type tooling for fine blanking.

Summary

The carbon supersaturation by the low temperature plasma carburizing is essential to protect the tool steel and high-speed tool steel punches and dies from adhesion wear during the forging and fine blanking of titanium and titanium alloy works. In particular, the free-carbon tribofilm, in situ formed on the YXR7 punch, minimizes the mechanical and chemical galling damages during the fine-blanking of titanium plates. Under the shearing stress transients in fine-blanking, this in situ solid lubrication plays a role to prevent the punch surfaces from severe galling. This tooling is available in the industries to continuously punch out the complex-shaped blanks of austenitic stainless steels, titanium and titanium alloys with fully burnished surfaces.

Acknowledgment

The authors would like to express their gratitude to S-I. Kurozumi (Nano-Film Coat, llc.) for his help in experiments.

References

[1] G.W. Kuhlman, Forging of titanium alloys, in: Metalworking: Bulk forming, Vol. 14 in ASM Handbook, 2005.

[2] M. Chandrasekaran, Forging of metals and alloys for biomedical applications, Ch. 10 in: Metals for biomedical devices, 2nd Ed. Woodhead Publishing, 2019, pp. 293-310.

[3] D.S. Fernández, B.P. Wynne, P. Crawforthc, K. Fox, M. Jackson, The effect of forging texture and machining parameters on the fatigue performance of titanium alloy disc components, Int. J. Fatigue 142 (2021) 105949. https://doi.org/10.1016/j.ijfatigue.2020.105949
[4] T. Kihara, Visualization of deforming process of titanium and titanium alloy using high speed camera, Proc. 2019-JSTP Conference 2019, pp. 41-42.
[5] S. Kataoka, M. Murakawa, T. Aizawa, H. Ike, Tribology of dry deep-drawing of various metal sheets wit use of ceramic tools, Surf. Coat. Technol. 178 (2004) 582-590. https://doi.org/10.1016/S0257-8972(03)00930-7
[6] K. Dohda K., T. Aizawa, Tribo-characterization of silicon doped and nano-structured DLC coatings by metal forming simulators, Manuf. Lett. 2 (2014) 82-85. https://doi.org/10.1016/j.mfglet.2014.03.001
[7] K. Dohda, M. Yamamoto, C. Hu, L. Dubar, K.F. Ehman, Galling phenomena in metal forming, Friction 9 (2020) 686-696. https://doi.org/10.1007/s40544-020-0430-z
[8] T. Aizawa, T. Yoshino, Y. Suzuki, T. Shiratori, Free-forging of pure titanium with high reduction of thickness by plasma carburized SKD11 dies, Materials 14 (2021) 2536. https://doi.org/10.3390/ma14102536
[9] T. Aizawa, T. Yoshino, Y. Suzuki, T. Shiratori, Anti-galling cold, dry forging of pure titanium by plasma-carburized AI-SI420J2 dies, Appl. Sci. 11 (2021) 595. https://doi.org/10.3390/app11020595
[10] T. Aizawa, T. Shiratori, In-situ solid lubrication in cold dry forging of titanium by isolated free carbon from carbon-supersaturated dies, J. Friction (2022) (in press).
[11] S. Ishiguro, T. Aizawa, T. Funazuka, T. Shiratori, Green forging of titanium and titanium alloys by using the carbon supersaturated SKD11 dies, Appl. Mech. 3 (2022) 724-739. https://doi.org/10.3390/applmech3030043
[12] T. Aizawa, T. Funazuka, T. Shiratori, Near-net forging of titanium and titanium alloys with low friction and low work hardening by using carbon-supersaturated SKD11 dies, Lubricants 10 (2022) 203. https://doi.org/10.3390/lubricants10090203
[13] T. Aizawa, Low temperature plasma nitriding of austenitic stainless steels, Ch. 3 in Stainless Steels and Alloys, IntechOpen, UK, London, 2019, pp. 31-50.
[14] D.M. Geobel, C. Becatti, I.G. Mikellides, A.L. Ortega, Plasma hollow cathodes, J. App. Phys.130 (2021) 050902. https://doi.org/10.1063/5.0051228
[15] J.J. Hong, W.C. Yeh, Application of response surface methodology to establish friction model of upset forging, Adv. Mech. Eng. 10 (2018) 1-9. https://doi.org/10.1177/1687814018766744
[16] K. Dohda, C. Boher, F. Rezai-Aria, N. Mahayotsanun, Tribology in metal forming at elevated temperatures, Friction 3 (2015) 1-27. https://doi.org/10.1007/s40544-015-0077-3
[17] S. Takeuchi, Treatise on the CVD diamond coatings, Ohm-Sha (2022).
[18] Y. Cao, F. Ernst, G.M. Michal, Colossal carbon supersaturation in austenitic stainless steels carburized at low temperature, Acta Mater. 51 (2003) 4171-4181. https://doi.org/10.1016/S1359-6454(03)00235-0
[19] R. Rementeria, J.D. Poplawsky, E. Urones-Garrote, R. D-Reyes, C. Garcia-Mateo, F.G. Caballero, Carbon supersaturation and clustering in bainitic ferrite at low temperature, Proc. 5th Int. Symp. Steel Science, Nov. 14, 2017, Kyoto, Japan, ISIJ (2017) 29-34.
[20] T. Aizawa, K. Fuchiwaki, Galling-free fine blanking of titanium plates using carbon supersaturated high-speed steel punch, J. Carbon Research (2023) (in press).
[21] T. Aizawa, T. Shiratori, Y. Kira, T. Inohara, Simultaneous nano-texturing onto a CVD-diamond coated piercing punch with femtosecond laser trimming, Appl. Sci. 10 (2020) 2674. https://doi.org/10.3390/app10082674
[22] T. Aizawa, T. Inohara, T. Yoshino, Y. Suzuki, T. Shiratori, Laser treatment of CVD diamond coated punch for ultra-fine piercing of metallic sheets, Ch. 4 in: Engineering Applications of Diamond, Intech Open, UK, London, 2021, pp. 43-65.